

EXPERIMENTAL STUDIES OF THE VIBRATION CHARACTERISTICS OF QUAY WALLS

by Satoshi Hayashi* and Nobuo Miyajima*

PREFACE

The principal cause of the difficulty of applying dynamical methods to the aseismic design of structures is the vagueness of the vibration characteristics of structures.

In order to acquire the fundamental data for dynamical methods of the aseismic design by the investigation of vibration characteristics of quay walls, we have performed a series of vibration tests of various types of prototype quay walls. In this paper, we intend to report the results of experiments and additional analytical considerations.

TRESTLE TYPE PIER

In many cases, trestle type pier can generally be considered as a relatively simple system of vibration. As for the No.7 pier in Kobe Port, we made a new attempt based upon a dynamical consideration, surmising first its vibration characteristics and then determining the distribution of seismic coefficients. As an objective of our vibration tests, two kinds of trestle type piers with completely different rigidity of supports were tested. The former was the trestle type pier with caisson studs and the latter was the trestle type pier with pilings.

I. Trestle type pier with caisson studs.

As an example of this type of pier, we have performed a vibration test of No.7 pier in Kobe Port. This pier is located in the eastern part of Kobe Port, and has a shape of twin pier consisting of the west and the east side pier. Each pier has dimensions of 51.8 m in width and 200 m in length, and is divided into four blocks of 50 m long. Each block is set on nine caisson pier studs. On these trestle type piers, are constructed super structures (i. e. warehouses and soilos), the shapes of which are different between the west and the east piers as shown in the Fig. 1 (a), (b).

To determine the seismic coefficient for the design of this pier, two kinds of new attempts were made. One of these is that we determined the intensity of ground vibration taking the characteristics of the earthquake motion based upon the geological formation into consideration (1). Next, for the determination of the distribution of seismic coefficient of structure, we assumed a block of the pier to be a vibration system with uniform density and rigidity, and also assumed that the shear vibration of the first order would be predominant during earthquake. In this way, the vertical distribution of seismic coefficients of the structure is indicated by the following formula (2) where; α_0 denotes the average seismic

$$\alpha(x) = \frac{\pi\alpha_0}{2} \sin \frac{\pi x}{2l} \quad (1)$$

* Soil Mechanics Division, Transportation Technical Research Institute, Ministry of transportation, Japanese Government.

coefficient of the structure, X denotes the coordinate of vertical direction taking positive upwards, and L denotes the whole height of the structure. The seismic coefficients for the design of this pier was determined as shown in the Table-1, based upon the formula (1).

With the principal purpose of checking the distribution of seismic coefficients determined in this way, the following four kinds of vibration tests of prototype pier were held; 1) Measurement of free vibration caused by sudden release of the structure from initial tension, 2) Measurement of forced vibration by vibrator, 3) Measurement of forced vibration by the explosion of dynamites set on the sea bottom, and 4) Measurement of forced vibration by natural earthquakes. The principal results of these tests were as follows.

1. Free vibration.

Measurements of free vibrations were made at the second block of the west pier. Free vibrations were initiated by pulling the pillars of warehouse by ropes attached to a tug boat, and then releasing the rope tension by cutting. By supplementary computations of vibrograms acquired in this way, the period of free vibration of the first order of this block was determined as 0.44 sec and the damping coefficient was 16% of critical damping (3).

2. Vibrator tests.

Vibrator tests were made at the second block of the west pier as the measurements of free vibrations. The vibrator used in this test could generate the vertical or horizontal sinusoidal centrifugal force by revolution of four discs with eccentric masses, and the maximum centrifugal force was about three tons. The vibrator was placed on the centre of the third floor, and we had the vibrogram of each floor of the pier by the horizontal centrifugal force perpendicular to the axis of the pier. From resonance curves (3) and deflection curves (3) in resonance acquired by the vibrograms above mentioned, the periods of free vibration of the second order and the fourth order were determined as 0.12 sec and 0.05 sec respectively. The first and the third order resonance could not be obtained.

3. Explosion tests.

Explosion tests were performed at the west and the east pier of No.7 pier and No.8 pier which has the same structural type with No.7 pier. Explosives were set on the sea bottom which were 400~1600 m distant from the pier in the direction perpendicular to the axis of the pier, and the charges of explosives were 4.5~27 kg. At one test, dynamites (about 10 kg) were exploded at the sea bottom about 800 m distant from the pier on the stretch of the pier axis.

According to the results of preliminary test, it was found that the amplitudes of vibration of axial component were smaller than those of perpendicular component to the pier axis, and on the modes of vibration projected to horizontal plane, neither torsion nor rotation had been observed but only translation. By combining vibrograms of the horizontal and vertical components of vibrations, it was found that rocking motion of the pier occurred because of the deformation of foundation soil.

The principal purpose of the explosion tests was to measure the

horizontal acceleration (component of cross sectional direction) of each floor and ground, and to compare the distribution of seismic coefficients for design with the data derived from explosion tests. According to the results of the explosion tests, the maximum acceleration at the top of the piers was 5-6 times greater than the ground acceleration. The cause of this phenomenon is probably that the period of ground vibration induced by explosion is close to the period of free vibration of the first order of the structure.

4. Measurements of vibration of the pier caused by natural earthquakes.

In order to have a knowledge of the behaviour of vibration of the pier caused by such irregular ground motion as the earthquake motion, measurements of vibration had been performed for about a year beginning in the April of 1955 by electromagnetic seismographs (4) set on each floor of the west pier. An example of the results of measurement are shown in Figure 3 (a) (b). Figure (3) shows distribution of amplitudes at each floor, and the wave groups in the figure are wave trains with similar periods and of comparatively regular shape. The periods obtained were longer (0.4 sec ~ 0.9 sec) with the number of waves of similar periods being less than obtained from the explosion test. The ratio of amplitudes, at the roof level to those at the bottom of the pier is smaller here than it was in the explosion test.

To confirm and generalise the experimental results by some analytical considerations, we conceived a simplified model of the pier and computed the response of the model by an earthquake. The model of the pier used, as shown in Fig. 4, was a system of four particles corresponding to the system of shear vibration of continuous body.

In this model, we assumed that the masses M_i concentrated to each floor, while to determine the rigidity of each floor K_i , we used the following formula (2).

$$S_i = \sum_{j=1}^4 M_j \ddot{\xi}_j = K_i (y_i - y_{i-1}) \quad (2)$$

where, S_i denotes the shear of i th floor. The formula (2) is applicable to cases of the resonance of the first order, and approximately speaking, the vibration of the structure caused by the explosion considered to be the resonance of the first order. Consequently the acceleration of each floor to the coordinate at rest $\ddot{\xi}_i$ and the relative displacement to the ground motion y_i can experimentally be obtained. Using these experimental data, constants of the model are obtained as shown in Table-2, and then the period and mode $\beta_i \phi_i^{(n)}$ of free vibration of each order can be calculated. (see Fig. 5).

In order to examine the adaptability of the model system of particles, forced vibration of this system have been computed. In this computation the acceleration of the bottom of the pier by explosion was used as a forcing function, (non-homogeneous term in differential equation) and the damping coefficient λ was tentatively set.

After introducing some modifications to the rigidity K_i of model system of particles as shown in the last column of Table-2, it was found that the computed and measured accelerograms of the roof (see Fig. 6) and the computed and measured results of vertical distribution of maximum

acceleration (see Fig. 7) well coincided, where damping coefficient h was 0.10 and the first order period of free vibration was 0.44 sec, the same as the result of free vibration.

Next, forced vibration of the model system of particles determined by the way mentioned above has been computed introducing the acceleration of an earthquake motion as a forcing function. Results of computations were shown in Fig. 8 and Fig. 9. In Fig. 8, earthquake ground motion y_0 and computed accelerogram of each particle ξ_i were shown, and the vertical distribution of max. acceleration was shown in Fig. 9. For these computations, DC electronic analog computer with arbitrary function generator was used. In order to represent the characteristics of the earthquake used for computations, the acceleration spectrum (5) of this earthquake was shown in Fig. 10.

As the vertical distribution of max. acceleration of simplified model of No.7 pier in an earthquake could be obtained, we made some comparison of distributions between various cases as shown in Fig. 11. According to the results as shown in Fig. 11, on the distributions of vibration of the pier by earthquakes, any remarkable difference between computed and measured results could not be recognised, and these distributions showed some different tendency from that of vibration caused by explosion and of seismic coefficients for design.

Within the scope of studying the vibration characteristics of the structure based upon the theory of linear vibration and considering the response of structure during earthquake, the distribution of max. acceleration of the pier in earthquakes was found as shown in Fig. 11, but for the purpose of studying the seismic coefficient for design itself, additional considerations on the other point of view must be useful.

II. Trestle type pier with reinforced concrete pilings.

The floor system of this pier is supported by long reinforced concrete piles, so the rigidity for lateral forces is smaller than that of pier with caisson studs above mentioned, but the trestle type pier constructed in Yokkaichi Port reported here is for the deep oil berth; moreover on the conditions of foundation soil there are thick and soft silty clay layers below the structure. So the vibration characteristics of this pier is worth noticing on the viewpoint of aseismic design.

This pier has the dimensions of 24 m in width and 219 m in length and is divided into three blocks as shown in Fig. 12 and Fig. 13.

The kinds of experiments performed were the vibrator test and measurements of free vibration as measured in No.7 pier above mentioned. The vibrator used here could generate the horizontal centrifugal force only (max.10 tons), and the vibrator was placed at the centre of each block. An example of resonance curves of each block derived from vibrator tests was shown in Fig. 14.

The main findings obtained by vibrator tests were as follows. (1) The amplitude of axial component of vibration of the pier was smaller than the amplitude of cross sectional component for unit centrifugal force. (2) According to the shapes of resonance curves, it was found that the non-linear

Vibration Characteristics of Quay Walls

restoring springs for lateral force of the pier might exist. (3) Effect of coupled vibration upon each block was recognised.

The measurement of free vibration was performed in the quite same way as mentioned in the test of No. 7 pier. An example of vibrograms derived from this test was shown in Fig. 15 (a), (b), (c). As in the case of vibrator test, effect of coupled vibration seemed to occur.

However it is supposed that the connection of each block of the pier would not be so strong, but each pier would move as an independent system of vibration during strong motion earthquake. For the simplicity of analysis, each block of the pier was regarded as an independent simple system of a particle with linear restoring spring, and the mechanical constants of systems were determined by the results of both kinds of experiments as shown in Table-3.

By the results of both vibrator test and measurement of free vibration, relationships between applied lateral forces and displacements of blocks of the pier were found as described in Fig. 16.

In order to have a knowledge of the behaviour of vibration of the pier during earthquake, we computed the response of each block of the pier to the same earthquake as in the analysis of No.7 pier in Kobe Port, by assuming each block as a simple system of a particle with the mechanical constants as shown in Table-3.

An example of the results of computations is illustrated in Fig. 17, (Which is for the first block, the farthest from the joining part to the land). It shows that the max. ground acceleration was 20 gals, while the max. acceleration of structure reached as much as 167 gals. Similarly for other blocks, the results show that the max. acceleration of structure was 103 gals on the second block and 73 gals on the third block.

We cannot give a definite conclusion of the tests, because the exact characteristics of the destructive earthquakes which would occur in this region and the variation of the characteristics of structure during such earthquakes are not entirely clear, but it may safely be supposed that the accelerations of blocks of the pier would be increased (especially in the farthest block from land) because of the fact that the damping coefficient is small and the period of free vibration is close to the period of probable earthquakes.

GRAVITY TYPE QUAY WALL

Gravity type quay walls are many and representative of all structural forms of quay walls. As an example of this type, vibration test on No.6 pier in Kobe Port has been performed. This pier has a shape of twin pier consist of two piers of the same shape, which has dimensions of 400 m in length and 54 m in width (cross section of the pier is shown in Fig. 18).

The principal items of measurements are as follows, (1) cross sectional distribution of acceleration, (2) axial distribution of acceleration, (3) vertical distribution of acceleration in the reclaimed land, and (4) measurement of elastic constants of soil in reclaimed land.

Explosion points were 1000 m (X) and 1500 m (Y) from No.6 pier in the direction of perpendicular to the axis of pier, and the charges of explosives were 11.25 kg (X) and 22.5 kg (Y).

According to result of seismic prospecting performed on the pier, the time distance curve indicating the formation of three layers was obtained, and the velocity of P-wave of each layer was 190 m/s (surface layer of dry sand in reclaimed land), 1350 m/s (saturated sand layer in reclaimed land), and 1850 m/s (original deposit) and the boundary of each layer seemed to be horizontal.

The principal results of the vibration tests of the pier were as follows.

(1) Cross sectional distribution of acceleration of the pier.

Displacement and acceleration seismographs (4) were set on the sea bottom and on the centre of axis of the pier in a straight line parallel to the cross section of the pier, and the vibration of horizontal motion occurred by explosion was measured. An example of results of the measurements is shown in Fig. 19 (a) by dots. These dots represent the ratio of max. acceleration to the max. ground motion acceleration (0.52 gals) of vibration of \perp ar (perpendicular to the axis of the pier) component caused by the explosion at Y.

(2) Axial distribution of acceleration of the pier.

Seismographs were set on the center line of the pier, and measurements were performed by the same way as mentioned above. The axial distribution of max. acceleration was as shown in Fig. 19 (b).

(3) Vertical distribution of acceleration in the reclaimed land.

Three holes with 3 m, 4.8 m and 7.7 m in depth were dug at the center of the pier, and by setting accelerographs at the bottom of holes, measurements of vibration caused by explosion were taken. Vertical distribution of max. acceleration of \perp ar component caused by explosion at Y was illustrated by dots in Fig. 19 (c).

If we could conceive a model of simple system of vibration with the same response and the same distribution of vibration as those obtained by the vibration test results on the pier, we should be able to compute also, by using this model, the response and the distribution of vibration at the time of an earthquake.

In contriving this model, soil in reclaimed land was regarded as uniform visco-elastic body, and with the behavior of gravity walls during vibration, it was assumed that rocking due to the deformation of subgrade would occur. And the pier consisting of the west and the east sub-piers was considered as one system of vibration.

The Equation of the motion of three dimensional visco-elastic body, considering the displacement of cross sectional component only, is as follows.

$$\frac{\partial}{\partial t} \left(\frac{\partial \bar{u}}{\partial t} + \frac{\partial u_0}{\partial t} \right) = (\lambda + 2\mu) \frac{\partial \bar{u}}{\partial x^2} + \mu \left(\frac{\partial^2 \bar{u}}{\partial y^2} + \frac{\partial^2 \bar{u}}{\partial z^2} \right) + (\lambda' + 2\mu') \frac{\partial^2 \bar{u}}{\partial t \partial x^2} + \mu' \left(\frac{\partial^2 \bar{u}}{\partial t \partial y^2} + \frac{\partial^2 \bar{u}}{\partial t \partial z^2} \right) \quad (3)$$

where; x, y, z denote the axes of coordinate parallel to the cross sectional, axial, and vertical directions of the pier respectively and in the same way a, c, l denote the dimensions of structure in the direction of x, y, z axes (see Fig. 20), u_0 and \bar{u} denote the amplitude of ground motion and relative displacement of structure to the ground in the direction of x -axis. Definitions of the other nomenclatures are as follows, λ, μ : elastic constant; λ', μ' : coefficient of viscosity; $\bar{\rho}$: bulk density; g : acceleration of gravity.

First we consider the boundary conditions. At $x=0$ and $x=a$, i.e. at both ends in x -direction, gravity type walls support the reclaimed soil, but the walls will have some movements because of earth pressure when vibration takes place. It was assumed that the rotation centre of the movements of the walls was located at the base of the walls, and the resistance against rotation was subgrade reaction. We can assume therefore that the relative displacement \bar{u} will take place due to the rotation throughout the range $0 \leq x \leq a$. So, \bar{u} will be written as follows

$$\bar{u}(x, y, z, t) = \theta(x, y, t) \cdot f(z) = \theta z \quad (4)$$

where, θ denotes the angular displacement. Then the overturning moment acting upon walls induced by earth pressure around the base will be written as follows, if the viscosity of soil is not taken into account.

$$\int_0^a (\lambda + 2\mu) \frac{\partial \bar{u}}{\partial x} \cdot z \, dz = (\lambda + 2\mu) \frac{l^3}{3} \frac{\partial \theta}{\partial x} \quad (5)$$

While the resisting moment against overturning acting upon the base of the walls is written in the following formula.

$$\int_{-\frac{b}{2}}^{\frac{b}{2}} k_s \theta x^2 \, dx = \frac{b^3}{12} k_s \theta \quad (6)$$

where, b denotes width of wall and k_s is the coefficient of subgrade reaction (6). (see Fig. 21)

Thus, the boundary conditions can be written as follows.

$$(i) \text{ at } x=0 \quad \frac{b^3}{12} k_s \theta = (\lambda + 2\mu) \frac{l^3}{3} \cdot \frac{\partial \theta}{\partial x} \quad (7)$$

$$(ii) \quad x=a \quad \frac{b^3}{12} k_s \theta = -(\lambda + 2\mu) \frac{l^3}{3} \cdot \frac{\partial \theta}{\partial x} \quad (8)$$

$$(iii) \quad y=0 \quad \bar{u}=0, \text{ i.e. } \theta=0 \quad (9)$$

$$(iv) \quad y=c \quad \bar{u}=0, \quad \theta=0 \quad (10)$$

$$(v) \quad z=0 \quad \bar{u}=0, \quad f(z)=0 \quad (11)$$

$$(vi) \quad z=l \quad \frac{\partial \bar{u}}{\partial z}=0, \quad \frac{df}{dz}=0 \quad (12)$$

Now, the solution of equation (3), when the ground motion $u_0(t)$ is the arbitrary function with irregular shape under the boundary conditions above mentioned, is as follows.

$$\ddot{u} = \sum_i \sum_m \sum_n \frac{(-1)^{m+1} 96 \{a^2(1-\cos\delta_i) + K\delta_i a \sin\delta_i\}}{\pi^3 \delta_i (2m-1)(2n-1)^2 (K\delta_i^2 + 2Ka + a^2)} \left(\sin \frac{\delta_i x}{a} + \frac{K\delta_i}{a} \cos \frac{\delta_i x}{a} \right) \frac{\sin(2m-1)\frac{\pi y}{a} \sin \frac{(2n-1)\pi z}{2\ell}}{a} \\ \times \frac{1}{P_{i,m,n} \sqrt{1 - h_{i,m,n}^2}} \int_0^t \ddot{u}_0 e^{-h_{i,m,n} P_{i,m,n} (t-\tau)} \sin P_{i,m,n} \sqrt{1 - h_{i,m,n}^2} (t-\tau) d\tau \quad (13)$$

(i=1,2,3,..., m=1,2,3,..., n=1,2,3,...)

where;

$$\left. \begin{aligned} \tan \delta_i &= \frac{2K\delta_i}{a} \left(\frac{K\delta_i}{a} \right)^2 - 1, & K &= \frac{4(\lambda+2\mu)}{k_s} \left(\frac{\ell}{b} \right)^3 \\ P_{i,m,n} &= \sqrt{\left(\frac{c_1 \delta_i}{a} \right)^2 + \left\{ \frac{(2m-1)G\pi}{c} \right\}^2 + \left\{ \frac{(2n-1)C_2\pi}{2\ell} \right\}^2}, & C_1 &= \sqrt{\frac{(\lambda+2\mu)g}{r}}, & C_2 &= \sqrt{\frac{\mu g}{r}} \\ h_{i,m,n} &= \frac{1}{2P_{i,m,n}} \left[\left(\frac{c_1 \delta_i \nu_1}{a} \right)^2 + \left\{ \frac{(2m-1)G\nu_2\pi}{c} \right\}^2 + \left\{ \frac{(2n-1)C_2\nu_3\pi}{2\ell} \right\}^2 \right], & \nu_1^2 &= \frac{\lambda+2\mu'}{\lambda+2\mu}, & \nu_2^2 &= \frac{\mu'}{\mu} \end{aligned} \right\} (14)$$

We conducted numerical computations of eq. (13) using numerical values illustrated in Table-4 and regarding the acceleration of ground motion induced by the explosion as a forcing function. In these computations, vibration of the first order mode only in all directions was taken into consideration, and the value of damping coefficient h was variously set. And by eq. (14), we obtained 0.32 sec for the period of free vibration of the first order of the pier, making use of the numerical values as shown in Table-4. An example of the results of computations with acceleration of ground motion induced by explosion at Y being taken into consideration as a forcing function was shown in Fig. 19 (a), (b), (c). As with the case of the results of the tests, the ratios of the max. acceleration of each point to the max. ground acceleration were indicated there. Considering throughout the whole results of computations by explosions at X and Y, it was found that the computed and measured results of the distribution of the max. acceleration best coincided when the damping coefficient h was set at 0.25.

Response and distributions of acceleration caused by an earthquake can be obtained by the same computations as mentioned above, considering the earthquake ground motion (same as used in the computation of No.7 pier) as a forcing function and $h=0.25$. Results of these computations are illustrated in Fig. 22 (a), (b), (c).

In this way, we could have a knowledge of the behaviour of vibration of the pier with gravity type quay walls during earthquake regarding the reclaimed soil as a visco-elastic body, but because there were no results of the natural frequency and the damping coefficient of the structure obtained from direct measurement, the examination of adaptability of the simplified model of gravity type quay walls was not so completely performed as with the trestle type pier. Moreover, it is supposed that the variation of the vibration characteristics of earth-retaining structures like this during a strong earthquakes, will be greater than that of the trestle type pier.

CELLULAR QUAY WALL

There are many problems to be made clear for aseismic design of cellular quay wall. In order to have knowledge on the following items among others,

Vibration Characteristics of Quay Walls

vibration test of prototype cellular quay wall in Tobata Harbour, Yawata Iron & Steel Co., was conducted, (1) distribution of vibration and response of structure to the ground motion, (2) earth pressure acting upon walls and variation of hoop tension of sheet-piles during an earthquake. The cross section of quay walls is shown in Fig. 23. Regarding the geological condition of this site, there are tertiary sand stone below the structure.

The kind of vibration test performed here was explosion test. Explosives (4.5 kg ~ 112.5 kg) were set at the sea bottom 350 m (W), 500 m (X) and 900 m (Y) distant from the structure. In this test, electro-magnetic seismographs (4), Carlson-type strain meters and earth pressure meters were used. These Carlson-type strain and stress meters had been set at the sheet piles of No.8 and 9 cells before vibration test. As the fill materials of the cell of this quay wall slags were used except No.9 cell in which sand was filled.

Relationships between the acceleration of the horizontal motion of vibration of each part of structure in the direction perpendicular to the normal line and that of ground motion vary according to the amount of charges of explosives and the distance from explosion point as shown in Fig. 24 (abscissa shows the distance from the normal line of quay wall and ordinate shows the max. acceleration of each station). As a general trend, the acceleration of ground motion is greater than that of the structure, but the amount of the charges and the distances from the explosion points become greater, the ratio of the acceleration of the structure and that of ground motion also increases. The cause of these results is probably that the predominant period of vibration induced by explosion increases and approaches to the natural period of structure when the charges and distances from explosion points increase.

The period of free vibration of this structure could not be obtained by direct measurement, but by the comparison between acceleration spectrum (5) of vibration on the structure and that of ground motion, it will be supposed that the natural period of structure is about 0.15 sec.

It is difficult to surmise the behaviour of vibration of cellular quay wall during an earthquake because characteristics of earthquake which may occur in this area are still not well known, but if they should be the same as given in the preceding sections, it may be supposed that intensity of vibration of the structure will be uniform and the same as ground motion.

According to the results of measurements of hoop tension, it was at most 2% of the initial value during vibration for the acceleration 10 gals on the quay wall. Relationship between the variation of hoop tension and the acceleration of the structure during vibration is not so clear, but it is inconceivable that the cell will be burst by an earthquake with the same intensity as the seismic coefficient for the design of this structure ($\alpha = 0.05$).

Next, the average value of variation of earth pressure in fill materials during vibration, which is the determining factor in shear deformation of the cell will be smaller than the variation of hoop tension at the point discussed above, because the phase difference between each part is likely to exist. And the earth pressure acting behind the wall could not be observed in this test.

CONCLUSION

According to the vibration test results on constructed prototype quay walls and some additional analytical considerations upon them, it would seem to be clear that these structures could be regarded as a relatively simple model system of vibration. Therefore we could presume the behaviour of structures during an earthquake by applying the theory of linear vibration. Thus it can be considered that fundamental data are here provided for introducing dynamical methods into the aseismic design of quay walls.

It should be noted, however, that as already mentioned, the vibration characteristics of the structures given in our test may change at the time of a strong earthquake, and the change again may not be uniform depending upon the type of the structure. Thus problems still remain for future research.

BIBLIOGRAPHY

1. "Determination of Seismic Factor for Structural Design of No.7 Pier of Kobe Port" by S. Hayashi and N. Miyajima, Report of Transportation Technical Research Institute, Vol. 1 No. 11-12.
2. "On the Vibration Characteristics of No. 7 Pier in Kobe Port." by S. Hayashi and N. Miyajima, unpublished.
3. "Aseismic Design of Quay Walls in Japan" by R. Amano, H. Azuma and Y. Ishii, Proceedings of the World Conference on Earthquake Engineering, June, 1956.
4. "On the Electro-magnetic Seismograph and its Dynamic Calibration" by S. Hayashi and N. Miyajima, Technical Note of Transportation Technical Research Institute, No.17.
5. "Spectrum Analysis of Strong Motion Earthquakes", by Alford J.L., Housner G.W. and Martel R.R., First Technical Report under O.N.R. Aug., 1951.
6. "Evaluation of Coefficients of Subgrade Reaction", by Karl Terzaghi, Geotechnique, Vol. 5, No. 4.
7. "A Few Considerations on the Earthquake Resistant Properties of the Harbour Pier," by M. Hatanaka, Transactions of the J.S.C.E., No. 44.

NOMENCLATURE

Explained as they first appear in the text.

Vibration Characteristics of Quay Walls

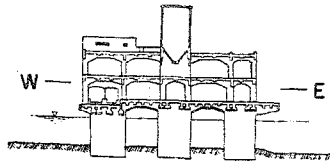
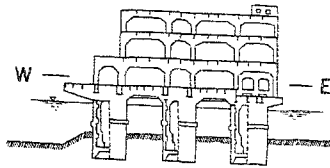


Fig. 1 Cross sections of No. 7 pier in Kobe Port.
a. The west side pier.
b. The east side pier.

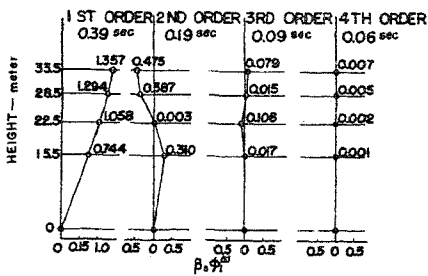


Fig. 5 Deflection curves in various modes of vibration.

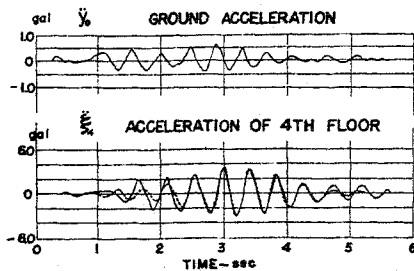


Fig. 6 Comparison between measured and computed accelerograms by explosion.

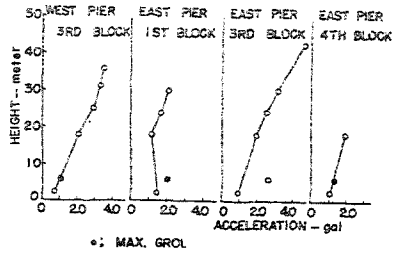


Fig. 2 Max. acceleration of each floor and ground induced by explosion.

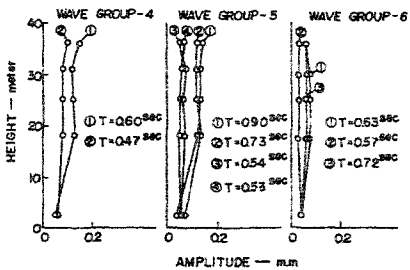
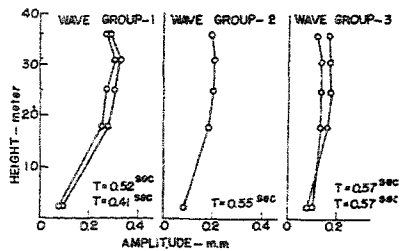


Fig. 3 Floor level displacements induced by a natural earthquake.

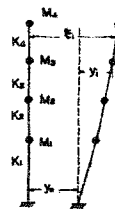


Fig. 4 Simple system of particles.

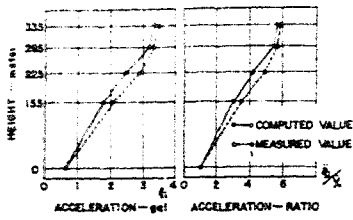


Fig. 7 Comparison between measured and computed distribution of max. acceleration by explosion.

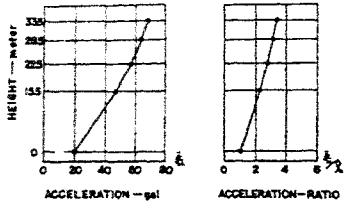


Fig. 9 Computed distribution of max. acceleration of each floor by an earthquake.

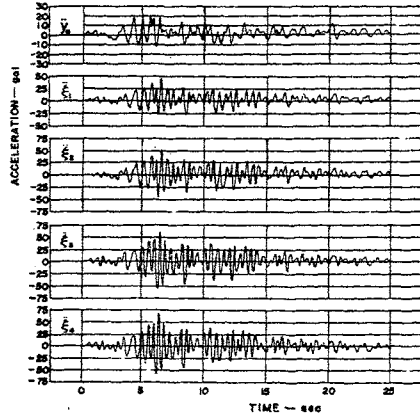


Fig. 8 Computed accelerograms of each floor of the pier by an earthquake.

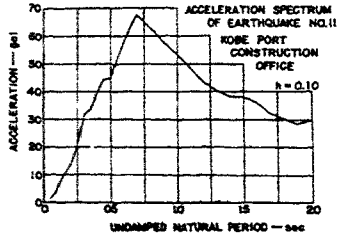


Fig. 10 Acceleration spectrum of the earthquake No. 11.

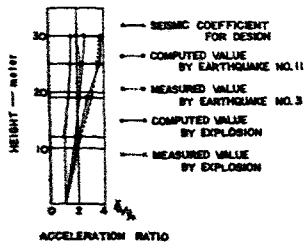


Fig. 11 Comparison between the distribution of seismic coefficient and various kinds of distributions of acceleration of each floor.

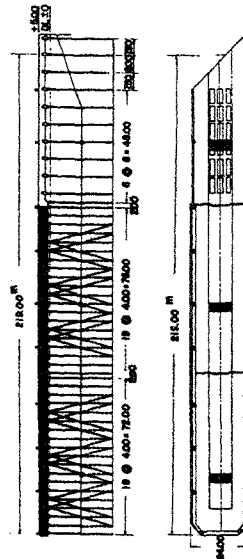


Fig. 12 Longitudinal section and plan of the trestle type pier with reinforced concrete pilings.

Vibration Characteristics of Quay Walls

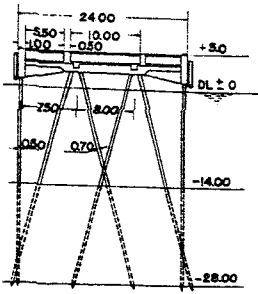
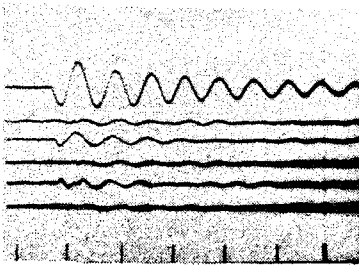
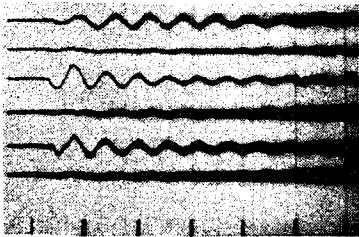


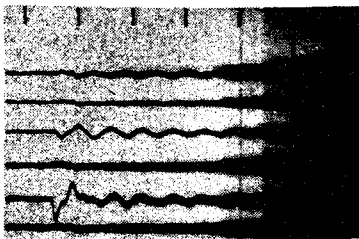
Fig. 13 Cross section of the trestle type pier with reinforced concrete pilings.



(a)



(b)



(c)

Fig. 15 Oscillograms of free vibration of each block.
a. 1st block.
b. 2nd block.
c. 3rd block.

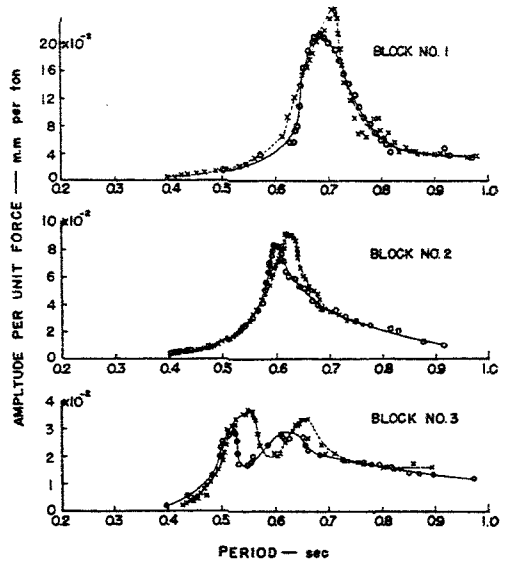


Fig. 14 Resonance curves derived from vibrator tests.

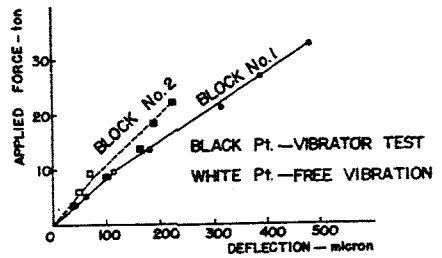


Fig. 16 Relationship between applied force and deflection of each block of the pier.

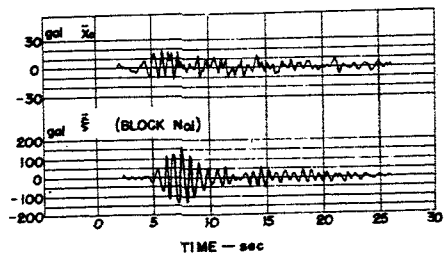


Fig. 17 An example of response computation of the first block of the pier in an earthquake.

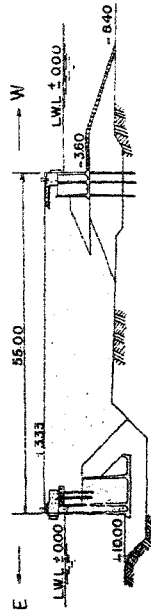


Fig. 18 Cross section of No. 6 pier in Kobe Port.

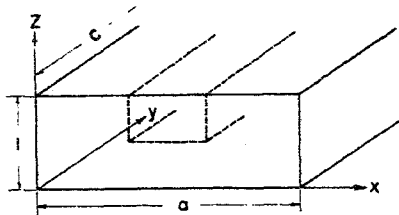


Fig. 20 Simple model of No. 6 pier in Kobe Port.

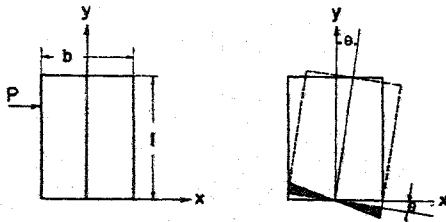


Fig. 21 Subgrade reaction of the gravity type wall.

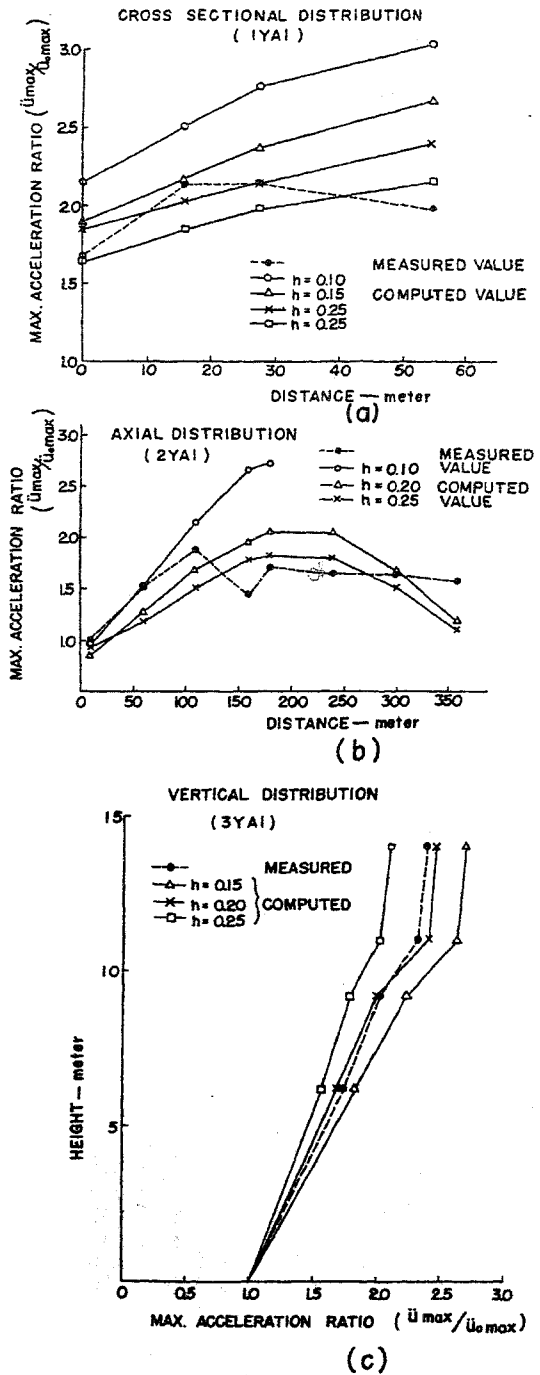


Fig. 19 Distribution of acceleration of No. 6 pier by explosion. a. Cross sectional distribution. b. Axial distribution. c. Vertical distribution.

Vibration Characteristics of Quay Walls

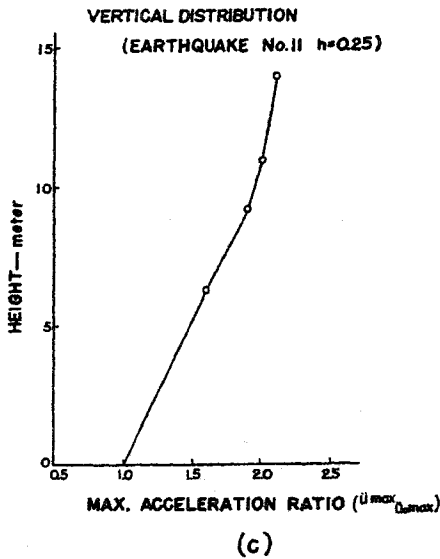
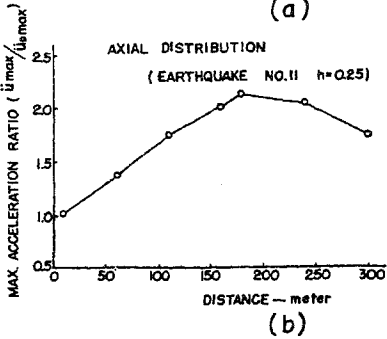
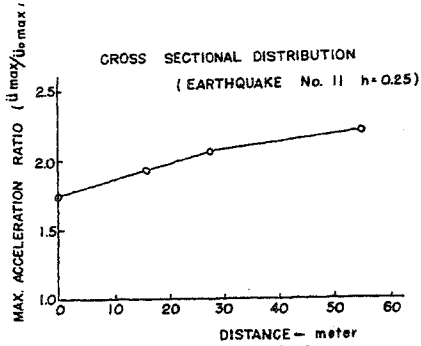


Fig. 22 Distribution of acceleration of No. 6 pier by an earthquake.
a. Cross sectional distribution.
b. Axial distribution.
c. Vertical distribution.

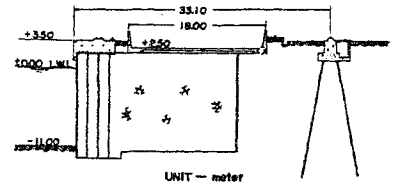


Fig. 23 Cross section of the cellular quay wall.

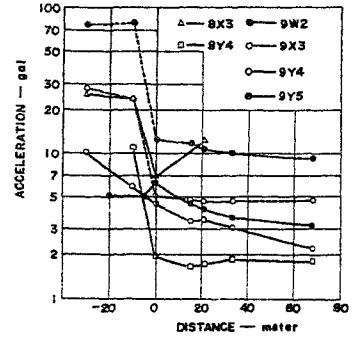


Fig. 24 Cross sectional distribution of max. acceleration of cellular quay-wall.

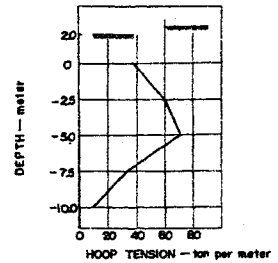


Fig. 25 Vertical distribution of hoop tension of the cell before vibration.

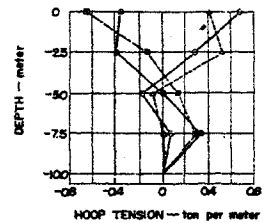


Fig. 26 Vertical distribution of variation of hoop tension during vibration.

Table 1
Seismic coefficient for design of No.7 pier in Kobe Port.

West side pier		East side pier	
1st floor	0.15	1st floor	0.15
2nd floor	0.20	2nd floor	0.20
3rd floor	0.23	roof	0.23
roof	0.24	silos	0.25

Table 2
Computation of rigidity of the west side pier.

floor No.	mass	acceleration	lateral force	displacement	deflection	rigidity	rigidity (modified)
i	M_i	$\ddot{\xi}_i$	$F_i = M_i \ddot{\xi}_i$	ξ_i	y_i	K_i^*	\bar{K}_i
	ton per gal	gal	ton	micron	micron	ton per cm	ton per cm
1	13.00	2.05	26.66	94.9	75.9	6840	5000
2	3.24	2.88	9.33	128.2	109.2	7590	5550
3	3.02	3.30	9.97	153.9	134.9	6040	4400
4	1.73	3.45	5.97	159.8	140.8	10120	7400
G				19.0			

$$* K_i = \frac{\sum_{n=1}^i F_n}{y_i - y_{i-1}}$$

Vibration Characteristics of Quay Walls

Table 3

The periods and circular frequencies of free vibration and the damping coefficients of each block of the trestle type pier with reinforced concrete pilings.

	period	circular frequency	damping coefficient
Block No.	T_0	$p = 2\pi/T_0$	h
	second	radian per sec.	
1	0.70	8.93	0.03
2	0.63	10.05	0.055
3	0.52	11.99	0.05

Table 4

Numerical values used in the computation of vibration of No.6 pier.

notation	unit	value	remarks
a	m	165	
b	m	10.3	
c	m	410	
l	m	14	
c_1	m/sec.	1350	from the result of seismic prospecting
c_2	m/sec.	130	from (7) in bibliography
δ	ton/m ³	2.0	
k_s	ton/m ²	37600	from (6) in bibliography

DISCUSSION

I. Sakamura, University of Tokyo, Japan:

Could you recognize some rocking phenomena at the vibration test of the trestle type quay wall?

S. Hayashi:

Yes, the rocking motion of the pier was observed in the explosion test of No. 7 Pier in Kobe Port and this should be considered in the precise analysis. We neglected, however, the effect of the rocking motion in our numerical computation to avoid the resulting complexity of computation. The results of computation showed good agreement with the measured value in spite of the approximation.

In the vibration test of the trestle type pier with reinforced concrete pilings, the measurement of rocking motion was not performed.